Hormetic Shifting of Redox Environment

by Pro-Oxidative Resveratrol Protects Cells Against Stress

Annabell Plauth[1], Anne Geikowski[1], Susanne Cichon[1], Sylvia J. Wowro[1], Linda Liedgens[1], Morten Rousseau[1], Christopher Weidner[1], Luise Fuhr[1], Magdalena Kliem[1], Gail Jenkins[2], Silvina Lotito[2], Linda J. Wainwright[2], Sascha Sauer[1,3,4*]

Affiliations

[1] Otto Warburg Laboratory, Max Planck Institute for Molecular Genetics, 14195 Berlin, Germany.

[2] Unilever R&D, Colworth Science Park, Sharnbrook, Bedfordshire, MK44 1LQ, UK.

[3] University of Würzburg, CU Systems Medicine, Josef-Schneider-Straße 2, Building D15, 97080 Würzburg, Germany

[4] Laboratory of Functional Genomics, Nutrigenomics and Systems Biology, BIMSB and BIH Genomics Platforms, Max-Delbrück-Center for Molecular Medicine, Robert-Rössle-Straße 10, 13125 Berlin, Germany

*Sascha Sauer
 Otto Warburg Laboratory
 Max Planck Institute for Molecular Genetics
 Ihnestrasse 63-73,
 14195 Berlin, Germany
 sauer@molgen.mpg.de
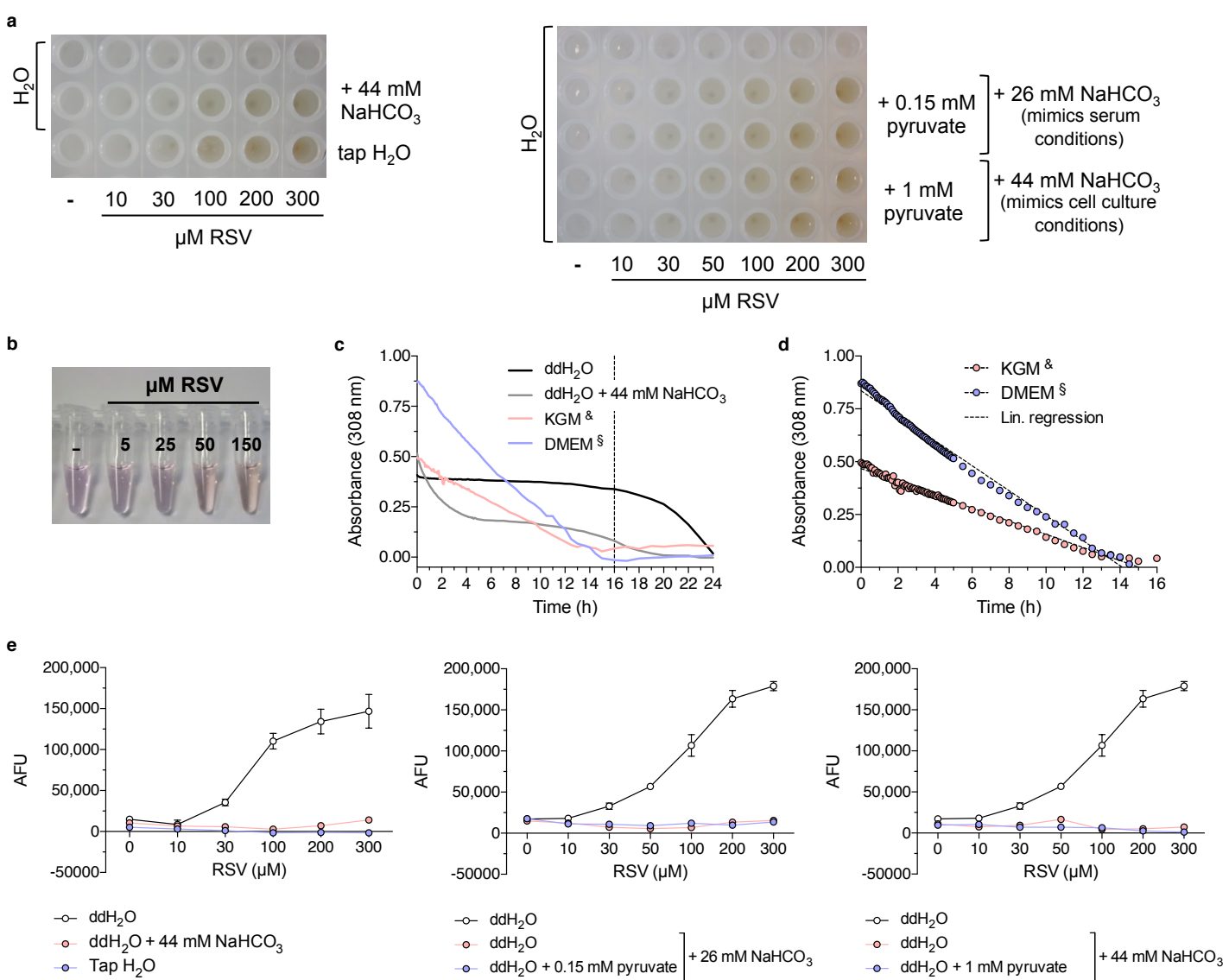
Fig. S1. Solvent-dependent stability of RSV. (a) Concentration-dependent colour change in diverse solvents mimicking physiological conditions after ~16 hours incubation with RSV. (b) Concentration-dependent colour change of cell culture medium (KGM, keratinocyte growth medium) due to 16 hours of incubation with RSV. (c) Kinetic measurement of light absorbance at maximum of RSV (308 nm) at 37°C in various solvents. Dotted line indicates putative beginning of evaporation. Detailed view on kinetic absorbance measurement from Fig. S1c (d). RSV reacts efficiently indicated by the linear and time-dependent decrease of absorbance. Values are mean (n = 3). See also Table S1. & 50 µM RSV, § 100 µM RSV. KGM, keratinocyte growth medium (e) Fluor-de-Lys assay to determine intact RSV after ~16 hours incubation. Values are mean ± s.e.m. (n = 4).
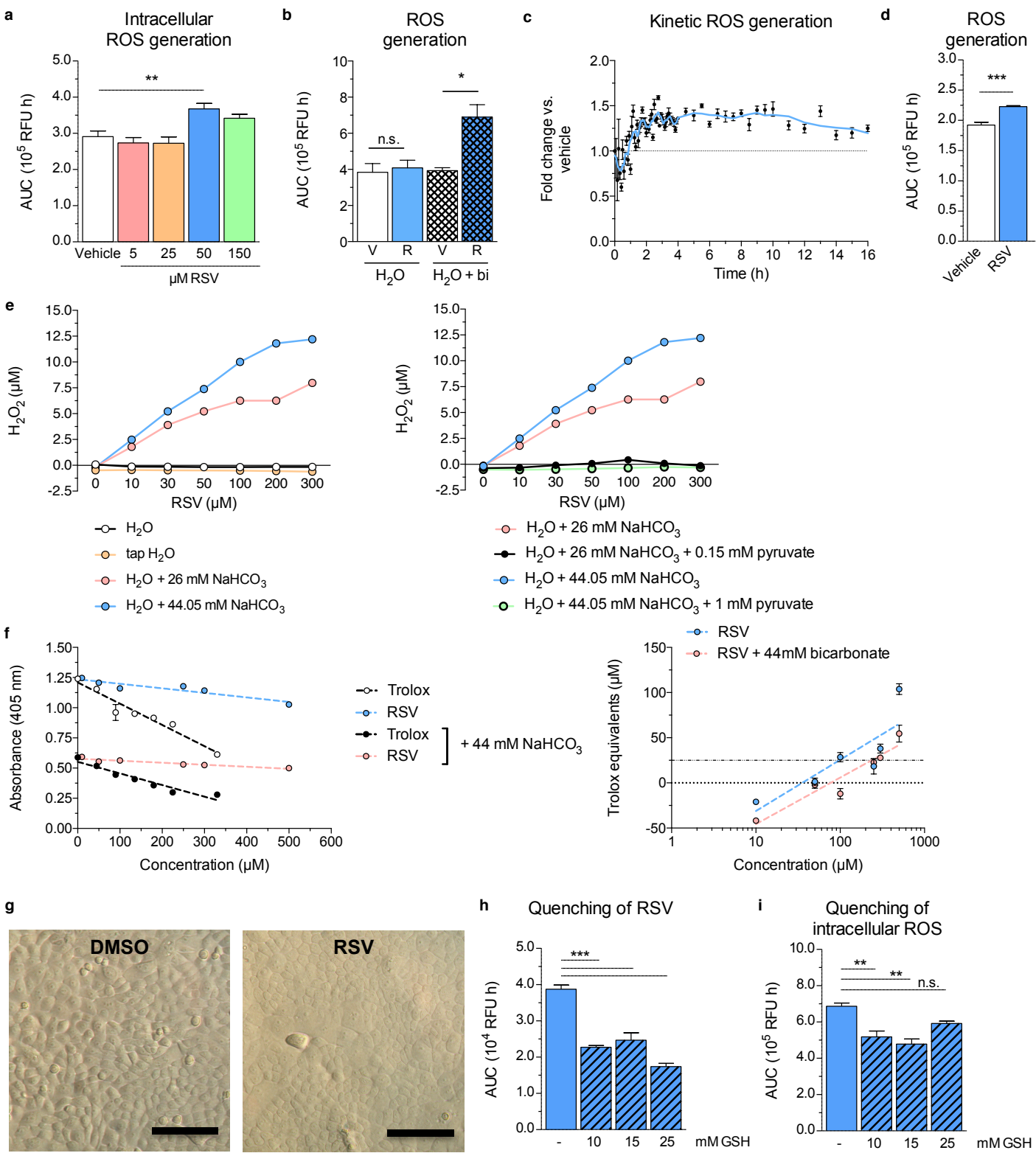
Fig. S2. RSV produces ROS, which can be diminished by $NaHCO_3$ and quenched by potent antioxidant GSH. (a) Intracellular ROS generation after 16 hours of RSV treatment of NHEK cells. Values are mean ± s.e.m. (n = 6), ** P < 0.01 one-way ANOVA versus vehicle. AUC, area under the curve. (b) Summed ROS generation in after incubation of vehicle (V) or RSV (R) in H_2O with or without 44 mM $NaHCO_3$ at 37°C (cell-free). Values are mean ± s.e.m. (n = 3). Bi, 44 mM $NaHCO_3$. (c and d) Kinetic (c) and summed (d) ROS generation derived from 50 µM RSV incubated in KGM (cell-free). Values are mean ± s.e.m. (n = 2-4). AUC, area under the curve. (e) H_2O_2 generation after 16.5 hours. Values are mean ± s.e.m. (n = 4). (f) Inhibition of ABTS oxidation by Trolox and RSV (left). 44 mM $NaHCO_3$ diminished antioxidant features of RSV roughly 2-fold (see dash-dot-dot line) (right). Values are mean ± s.e.m. (n = 3). (g) Macroscopical appearance of NHEKs treated with 50 µM RSV for 16 hours. Scale bar indicating 100 µm. (h and i) GSH considerably quenched RSV-driven ROS generation in KGM (cell free) (h) and in NHEKs (i). Values are mean ± s.e.m. ((h) n = 4; (i) n = 5), ** P < 0.01, *** P ≤ 0.001 one-way ANOVA versus RSV.
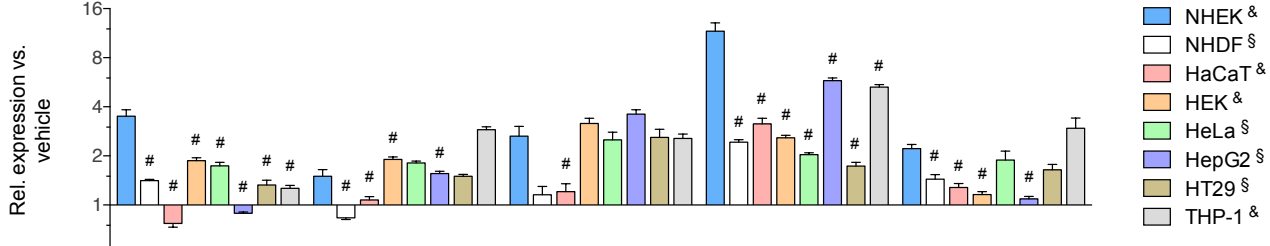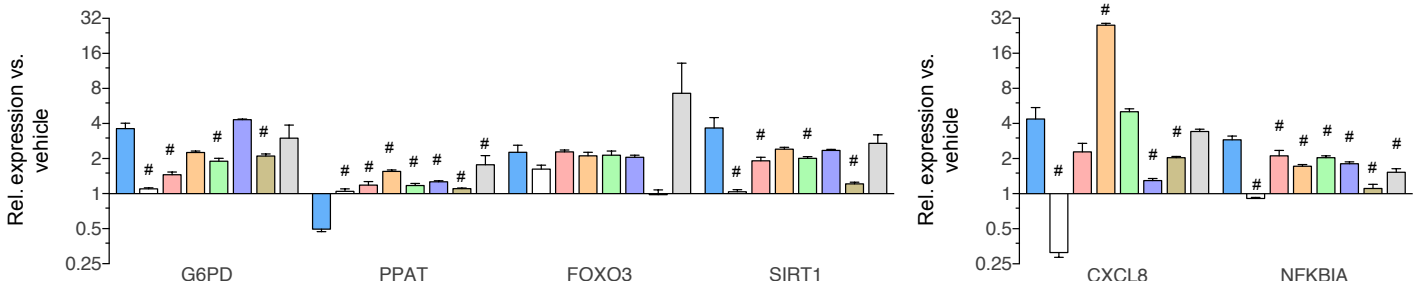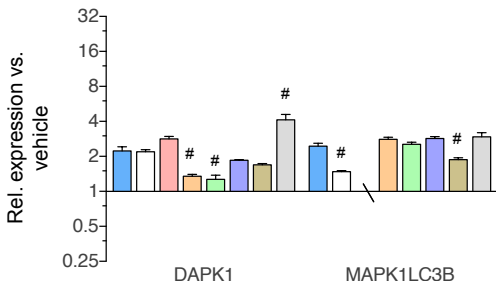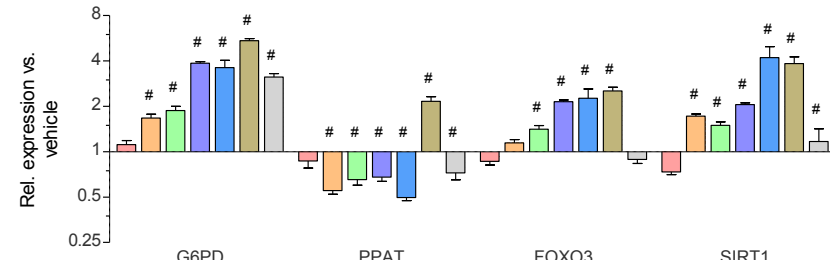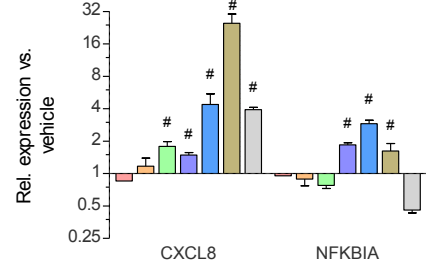
Fig. S3. RSV-driven expression of Nrf2 target genes observed in diverse cellular models and rarely concentration-dependent. (a, b, c and d) RSV effects are in principle similar for most cellular models tested. Values are ± s.e.m. (n = 4); # *P* <0.05 One-way ANOVA with subsequent Dunnett's post-test versus RSV-treated NHEKs. (e, f, g and h) The highest impact on gene expression without adverse effects is observed after 16 hours of treatment with 50 µM or 100 µM RSV. Values are mean ± s.e.m. (n = 4); # *P* < 0.05 versus vehicle. See also Figure 3a-d.
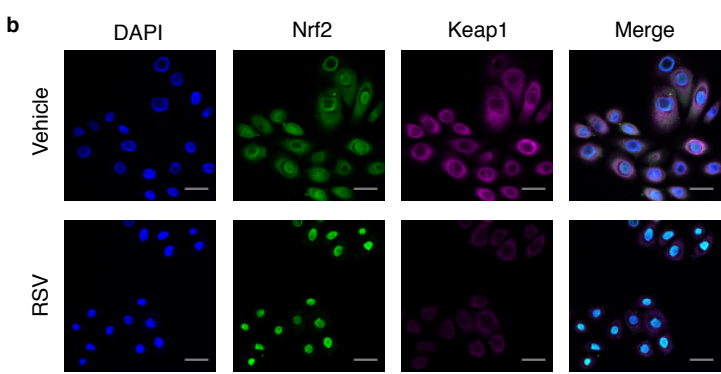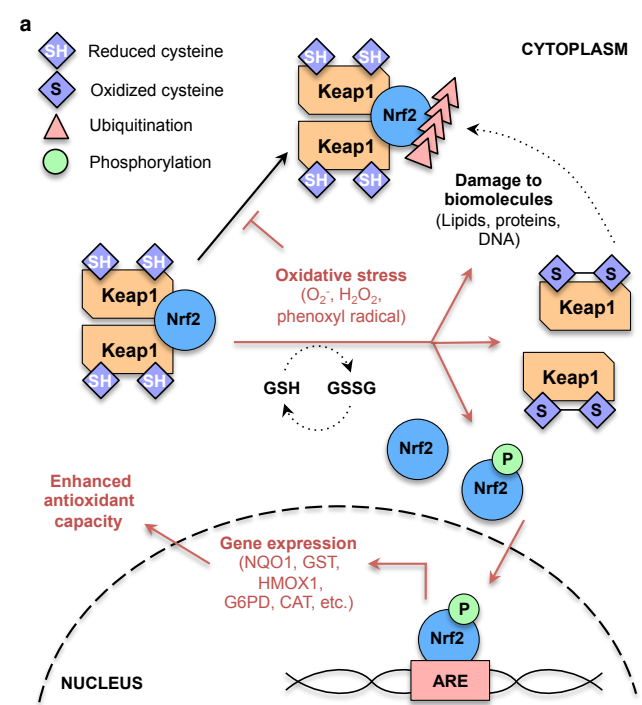
Fig. S4. The transcription factor Nrf2 mediates RSV effects. (a) Scheme of canonical Nrf2 signaling. Under physiological conditions Nrf2 resides in the cytoplasm as it is bound to its inhibitor Keap1, which facilitates ubiquitination via Cul3. Oxidative stress enables formation of bisulfide bonds in Keap1. Resulting conformational change of Keap1 triggers release of Nrf2, and its subsequent phosphorylation and translocation into the nucleus to enhance expression of anti-oxidative and other target genes. (b) Fluorescence staining marking DAPI (blue), Nrf2 (green) and Keap1 (magenta) in treated NHEKs. Scale bar equals 25 μm.
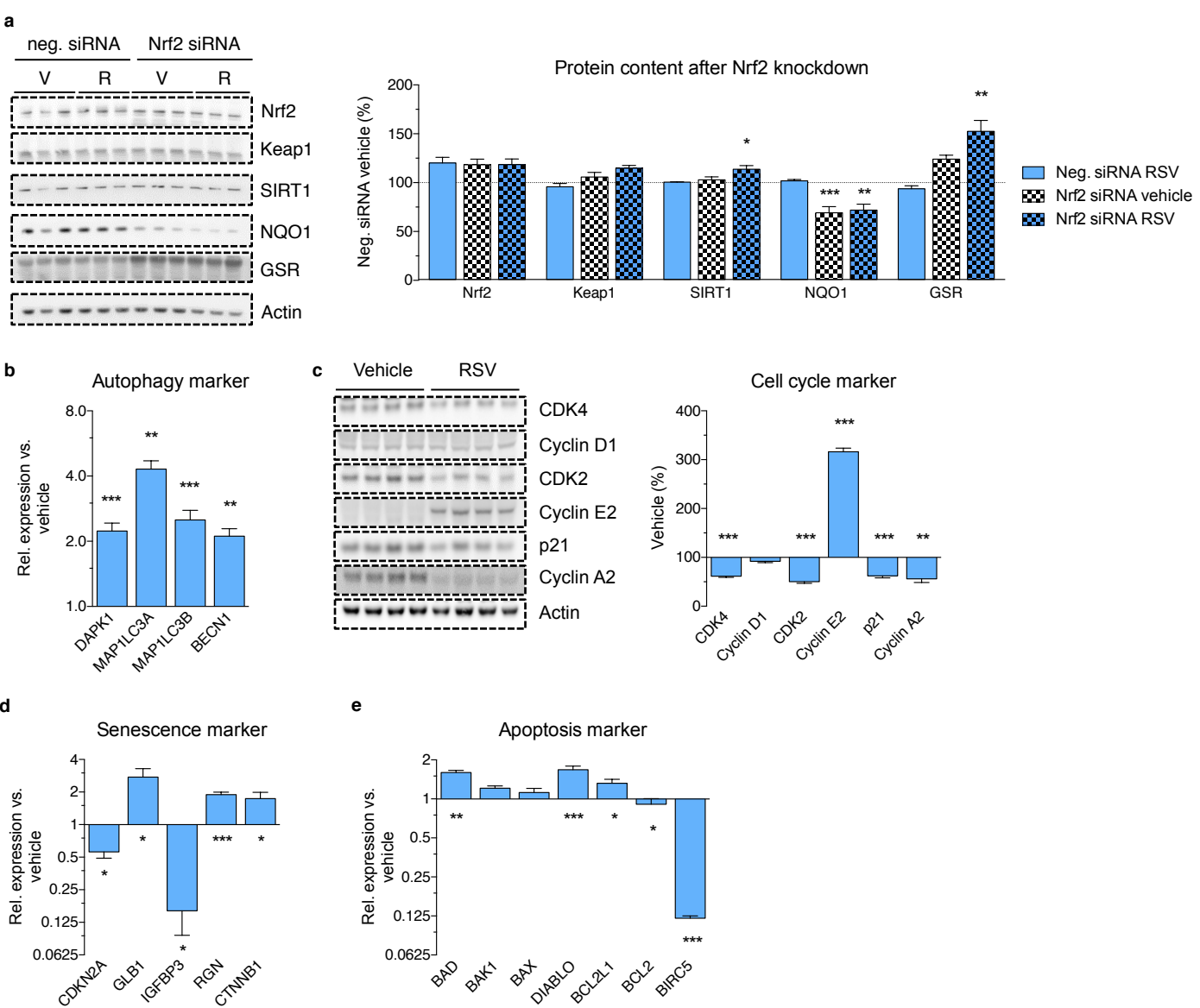
Fig. S5. Cellular effects of RSV are mediated by transcription factor Nrf2 and result in G1 phase cell cycle arrest. (a) Quantification of protein content upon Nrf2 knockdown in treated (50 µM RSV) NHEKs. Densitometric analysis was done relative to negative siRNA vehicle. All gels were run under the same experimental conditions and cropped blots depicted (copping: dashed line). Values are mean ± s.e.m. (n = 3); * $P < 0.05$, ** $P < 0.01$, *** $P ≤ 0.001$ one-way ANOVA versus negative siRNA vehicle. V, vehicle; R, RSV. (b) RSV substantially induced expression of autophagy marker genes in treated NHEKs. Values are mean ± s.e.m. (n = 4); ** $P < 0.01$, *** $P ≤ 0.001$ versus vehicle. (c) 50 µM RSV induced G1 phase arrest in treated NHEK cells. Densitometric analysis of immunoblots was done relative to vehicle. All gels were run under the same experimental conditions and cropped blots depicted (copping: dashed line). Values are mean ± s.e.m. (n = 4); * $P < 0.05$; ** $P < 0.01$, *** $P ≤ 0.001$ versus vehicle. (d) Senescence marker genes are diversely regulated in NHEKs by RSV treatment. Values are mean ± s.e.m. (n = 4); * $P < 0.05$, ** $P < 0.01$, *** $P ≤ 0.001$ versus vehicle. (e) RSV increased expression of pro-apoptotic genes while decreasing expression of anti-apoptotic BIRC5 in treated NHEKs. Values are mean ± s.e.m. (n = 4); * $P < 0.05$, ** $P < 0.01$, *** $P ≤ 0.001$ versus vehicle.
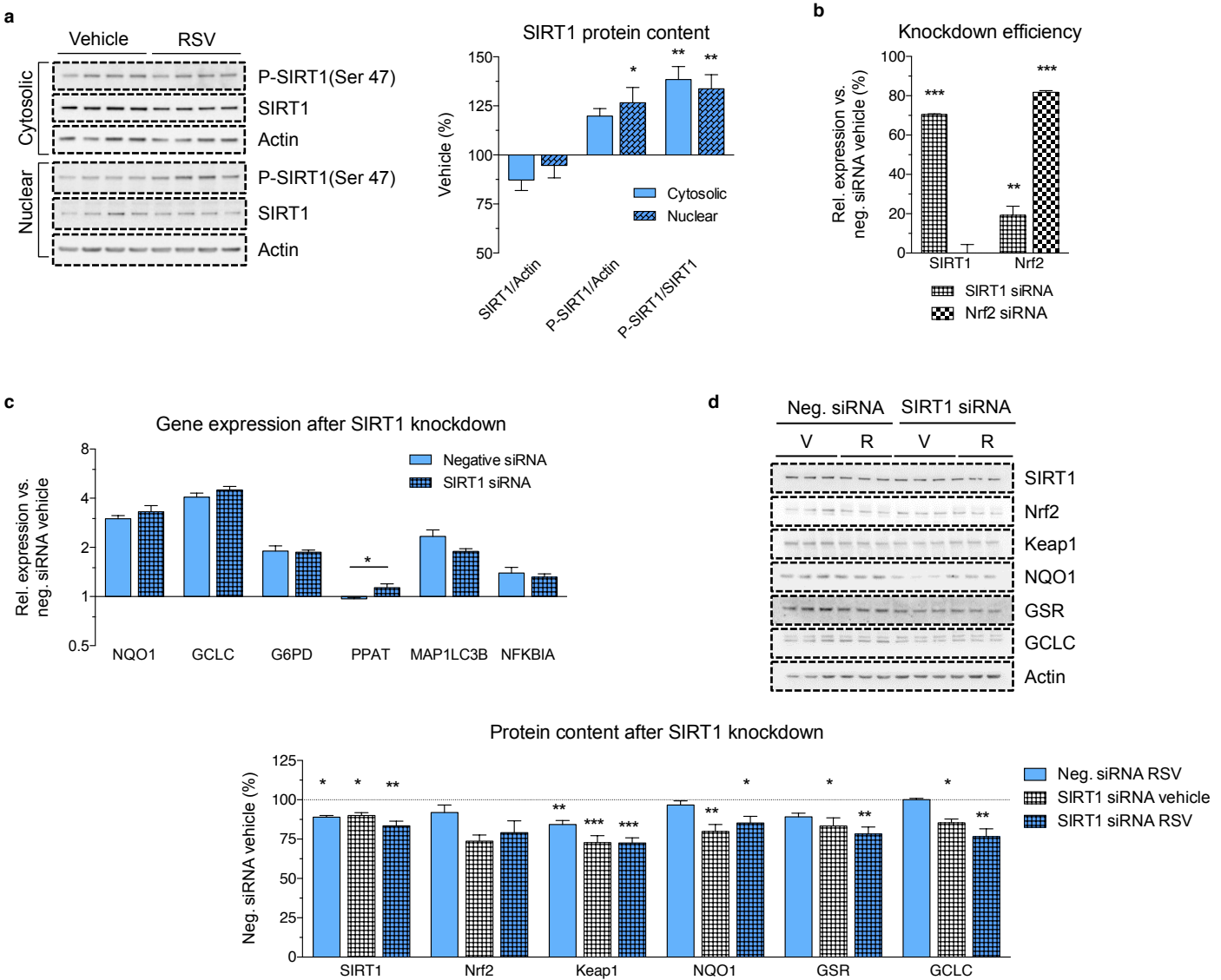
Fig. S6. Cellular effects of RSV are in part modulated by sirtuins. (a) Translocation of SIRT1 and increased amount of nuclear phosphorylated SIRT1 as well as SIRT1 protein. Densitometric analysis was done relative to vehicle. All gels were run under the same experimental conditions and cropped blots depicted (copping: by dashed line). Values are mean ± s.e.m. (n = 4); * P < 0.05, ** P < 0.01 versus vehicle. (b) Knockdown efficiency in RSV treated NHEKs. Knockdown of SIRT1 resulted in 20 % lower expression of Nrf2. are mean ± s.e.m. (n = 4); * P < 0.05 one-way ANOVA versus negative siRNA. (c) Quantification of gene expression upon knockdown of SIRT1 in RSV treated NHEKs. Values are mean ± s.e.m. (n = 4); * P < 0.05 one-way ANOVA versus negative siRNA vehicle. (d) Protein content upon knockdown of SIRT1 in RSV treated NHEKs. Densitometric analysis was done relative to negative siRNA vehicle. All gels were run under the same experimental conditions and cropped blots depicted (copping: dashed line). Values are mean ± s.e.m. (n = 3); * P < 0.05, ** P < 0.01, *** P ≤ 0.001 one-way ANOVA versus negative siRNA vehicle. V, vehicle; R, RSV.
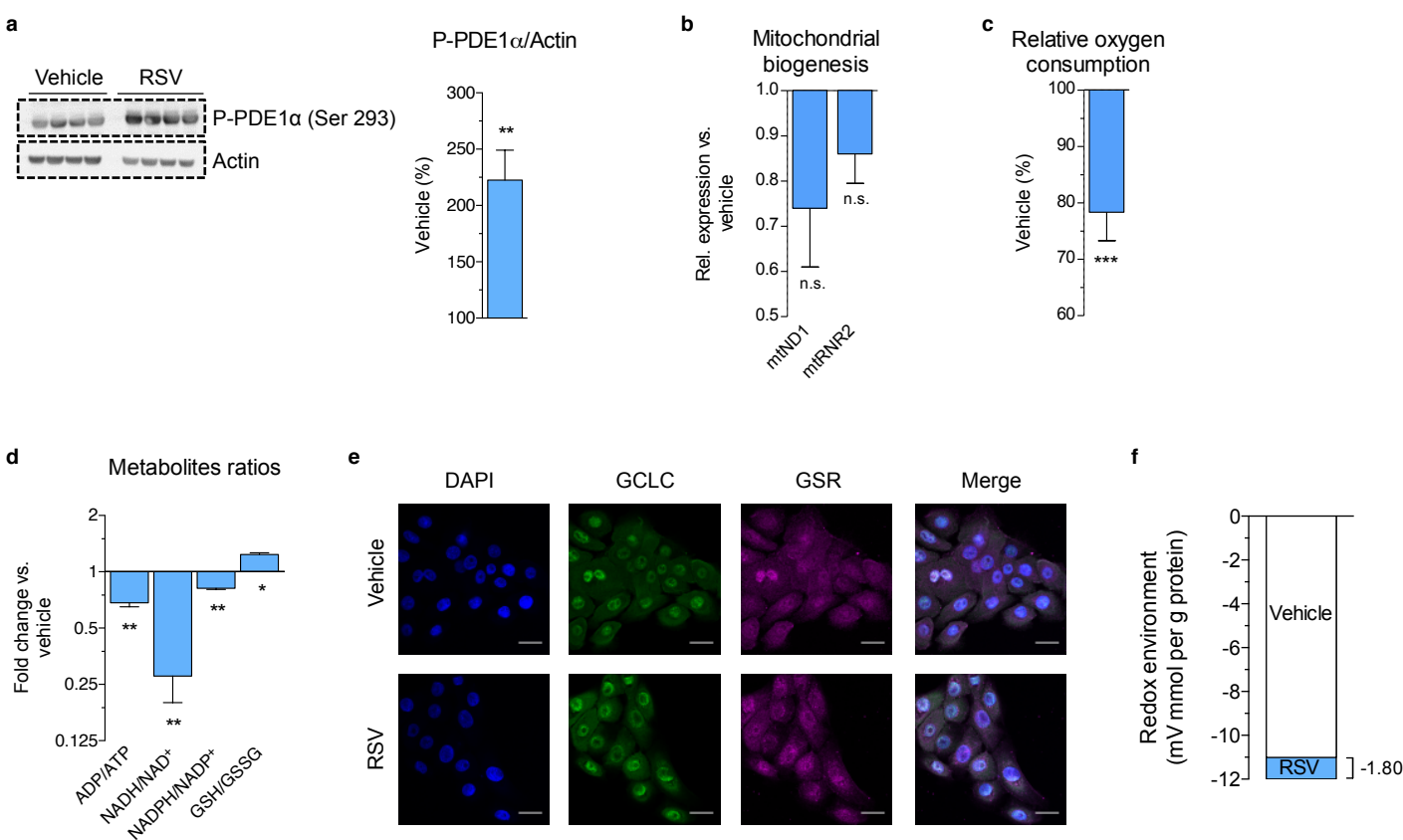
Fig. S7. RSV influences metabolite ratios, subsequently shifting the cellular redox environment to a reduced state. (a) RSV increased phosphorylation of pyruvate dehydrogenase subunit E1 α (PDE1α) at serine 293. Densitometric analysis was performed relative to vehicle. All gels were run under the same experimental conditions and cropped blots depicted (copping: dashed line). Values are mean ± s.e.m. (n = 4); ** $P < 0.01$ versus vehicle. (b) 50 μM RSV failed to induce mitochondrial biogenesis in RSV treated NHEKs. Values are mean ± s.e.m. (n = 4); n.s., not significant (c) RSV decreased mitochondrial oxygen consumption in RSV treated NHEKs. Values are mean ± s.e.m. (n = 8); *** $P \leq 0.001$ versus vehicle. (d) Calculated metabolite ratios (see Figure 5a); * $P < 0.05$, ** $P < 0.01$. (e) Fluorescence staining marking DAPI (blue), Glutamate-cysteine ligase catalytic subunit (GCLC, green) and glutathione-disulfide reductase (GSR, magenta) in RSV treated NHEKs. (f) Calculated redox environment considering all analysed metabolites. See also Table S4 and for GSH-based calculation Figure 5c.

Supplementary Material and Methods

Parameter	KGM[#]	DMEM[$]
Slope	-0.031 ± 0.0004	-0.059 ± 0.0007
Y-intercept (X=0.0)	0.467 ± 0.0027	0.836 ± 0.0043
X-intercept (Y=0.0)	15.04	14.15
R square	0.9844	0.9887
P value	< 0.0001	< 0.0001

Table S1. Linear regression of RSV degeneration in cell culture media. Results of the linear regression analyses of data presented in Fig. S1d. & 50 µM RSV, § 100 µM RSV. KGM, keratinocyte growth medium.

Name	NES	FDR q-val
SPLICEOSOME	-2.581	0.000
RNA DEGRADATION	-2.340	0.000
DNA REPLICATION	-2.239	0.000
CELL CYCLE	-2.143	0.000
LYSOSOME	2.160	0.000
SYSTEMIC LUPUS ERYTHEMATOSUS	2.110	0.001
METABOLISM OF XENOBIOTICS BY CYTOCHROME P450	1.882	0.015
STEROID HORMONE BIOSYNTHESIS	1.898	0.015
OTHER GLYCAN DEGRADATION	1.907	0.017
ADIPOCYTOKINE SIGNALING PATHWAY	1.847	0.021
PENTOSE AND GLUCURONATE INTERCONVERSIONS	1.821	0.025
PYRUVATE METABOLISM	1.777	0.029
PPAR SIGNALING PATHWAY	1.779	0.031
PEROXISOME	1.784	0.034
EPITHELIAL CELL SIGNALING IN HELICOBACTER PYLORI INFECTION	1.745	0.034
NATURAL KILLER CELL MEDIATED CYTOTOXICITY	1.732	0.035
GLUTATHIONE METABOLISM	1.750	0.036
NITROGEN METABOLISM	1.719	0.038
CYTOKINE CYTOKINE RECEPTOR INTERACTION	1.732	0.038
DRUG METABOLISM CYTOCHROME P450	1.691	0.043
RETINOL METABOLISM	1.699	0.044
PROXIMAL TUBULE BICARBONATE RECLAMATION	1.691	0.045
FATTY ACID METABOLISM	1.680	0.045
PURINE METABOLISM	-1.747	0.055
ARACHIDONIC ACID METABOLISM	1.647	0.060
PYRIMIDINE METABOLISM	-1.721	0.061
SPHINGOLIPID METABOLISM	1.637	0.062

TOLL LIKE RECEPTOR SIGNALING PATHWAY	1.626	0.066
PROPANOATE METABOLISM	1.620	0.067
GLYCINE SERINE AND THREONINE METABOLISM	1.587	0.087
VALINE LEUCINE AND ISOLEUCINE DEGRADATION	1.564	0.094
LIMONENE AND PINENE DEGRADATION	1.568	0.095
GLYCEROLIPID METABOLISM	1.572	0.095
BUTANOATE METABOLISM	1.552	0.097
FC EPSILON RI SIGNALING PATHWAY	1.557	0.097
STEROID BIOSYNTHESIS	1.530	0.102
TASTE TRANSDUCTION	1.526	0.103
B CELL RECEPTOR SIGNALING PATHWAY	1.533	0.103
CELL ADHESION MOLECULES CAMS	1.538	0.103
RNA POLYMERASE	-1.633	0.126
NOD LIKE RECEPTOR SIGNALING PATHWAY	1.467	0.152
ONE CARBON POOL BY FOLATE	-1.595	0.153
CHEMOKINE SIGNALING PATHWAY	1.459	0.157
GLYCOSAMINOGLYCAN BIOSYNTHESIS KERATAN SULFATE	1.445	0.167
PROTEASOME	-1.557	0.168
OOCYTE MEIOSIS	-1.568	0.170
AMINO SUGAR AND NUCLEOTIDE SUGAR METABOLISM	1.431	0.174
TRYPTOPHAN METABOLISM	1.426	0.175
ARGININE AND PROLINE METABOLISM	1.432	0.177
FC GAMMA R MEDIATED PHAGOCYTOSIS	1.420	0.178
INOSITOL PHOSPHATE METABOLISM	1.400	0.193
GLYCOSAMINOGLYCAN BIOSYNTHESIS CHONDROITIN SULFATE	1.401	0.197
PROGESTERONE MEDIATED OOCYTE MATURATION	-1.522	0.199
CITRATE CYCLE TCA CYCLE	1.382	0.212
BASE EXCISION REPAIR	-1.475	0.218
NUCLEOTIDE EXCISION REPAIR	-1.460	0.224
ECM RECEPTOR INTERACTION	-1.480	0.227
AMINOACYL TRNA BIOSYNTHESIS	-1.482	0.243

Table S2. Enriched KEGG pathways using (GSEA). Gene expression data were submitted to Gene Expression Omnibus database (GSE72119). GSEA was performed using parameters described in experimental procedures. Microarray data were analysed using the curated C2 KEGG pathways gene sets from the Molecular Signature Database. See also Figure 1e.

	NHEK[&]	NHDF[§]	HaCaT[&]	HEK[&]	HeLa[§]	HepG2[§]	HT29[§]	THP-1[&]
NHEK[&]		0.437	*0.610*	0.175	0.198	*0.502*	0.248	0.437
NHDF[§]	0.437		0.336	-0.321	-0.191	0.294	0.386	0.476
HaCaT[&]	*0.610*	0.336		0.235	0.428	*0.563*	0.201	*0.670*
HEK[&]	0.175	-0.321	0.235		*0.758*	-0.092	0.349	0.122
HeLa[§]	0.198	-0.191	0.428	*0.758*		0.388	*0.558*	0.223
HepG2[§]	*0.502*	0.294	*0.563*	-0.092	0.388		0.454	0.290
HT29[§]	0.248	0.386	0.201	0.349	*0.558*	0.454		0.155
THP-1[&]	0.437	*0.476*	*0.670*	0.122	0.223	0.290	0.155	

Table S3. Pearson correlation of gene expression data from diverse cell lines treated with RSV. Pearson correlation coefficients for data presented in Fig. S3a-d. Results with *P* values lower than 0.05 ($P < 0.05$) displayed in italic font. & 50 µM RSV, § 100 µM RSV.

Couple	$E^{0'}$ mV	e^-	H^+	$\Delta E/\Delta pH$	pH		E_{pH}		Reduced species (µmol per g protein)		Oxidized species (µmol per g protein)		n	$E_{hc,pH}$	
					DMSO	RSV	DMSO	RSV	DMSO	RSV	DMSO	RSV		DMSO	RSV
2GSH/GSSG	-240	2	2	-61.50	7.003	7.063	-240.16	-243.89	20.71	27.68	0.45	0.47	2	-331.79	-342.55
NADH/NAD$^+$	-320	2	1	-30.75			-320.08	-321.94	0.43	0.12	4.50	4.84	2	-288.85	-272.83
Lactate/pyruvate	-190	2	2	-61.50			-190.16	-193.89	18.88	16.90	3.56	4.87	2	-212.46	-210.49
NADPH/NADP$^+$	-320	2	1	-30.75			-320.08	-321.94	595,341	310,219	27,978	17,903	2	-360.91	-360.03

Table S4. Metabolites used to calculate the redox environment of the system. Values for NADPH and NADP (grey font) are relative fluorescence units (RFU). See also Fig. S7f and for GSH-based calculation Figure 5c.

Symbol	Gene ID	Forward primer	Reverse primer
ACTB	60	CAGCCATGTACGTTGCTATCCAGG	AGGTCCAGACGCAGGATGGCATG
BAD	572	TCCTTTAAGAAGGGACTTCCTCG	CAAGTTCCGATCCCACCAGG
BAK1	578	TGATTCAGCCAAATGCAGGG	GGTGAGGGGATTGCACAGTTT
BAX	581	CTTCTGGAGCAGGTCACAGT	GCAGGGTAGATGAATCGGGG
BCL2	596	GCGGCCTCTGTTTGATTTCTC	GTTGACTTCACTTGTGGCCC
BECN1	8678	CCGAGGTGAAGAGCATCGGG	TCGTGTCCAGTTTCAGGGGC
BIRC5	332	TGAGAACGAGCCAGACTTGG	TGTTCCTCTATGGGGTCGTCA
CAT	847	GCTTCAGGGCCGCCTTTTTGC	AGTTGGCCACTCGAGCACGG
CDKN2A	1029	GTGGACCTGGCTGAGGAG	CTTTCAATCGGGGATGTCTG
CTNNB1	1499	ACGGAGGAAGGTCTGAGGAG	TCAAATACCCTCAGGGGAACAG
CXCL8	3576	CTGATTTCTGCAGCTCTGTG	GGGTGGAAAGGTTTGGAGTATG
DAPK1	1612	GCAGCAGTTTGTGTACGACG	ATGTTGATCTCGCCTGTGCT
DIABLO	56616	CCACGCGGAGGTTGTAATTG	GTGTATTCTGCGATCTCGGC
FOXO3	2309	CTACGAGTGGATGGTGCGTT	TGTGCCGGATGGAGTTCTTC
G6PD	2539	GCCTCTTCTACCTGGCCTTG	GATGCGGTTCCAGCCTATCT
GCLC	2729	GAGGTCAAACCCAACCCAGT	TGTTAAGGTACTGAAGCGAGGG
GLB1	2720	CCGTGGGTCCTTAGTCAAGT	CAACAGAGGGAGGATGCGAA
GPX1	2876	TGTTGCTCGTAGCTGCTGAA	TGAGTCACCGGGATTTTGCC
GPX3	2878	CTGCTTTCCCTGCTCCTGG	ACCATGGCAGTCCATCTTCG
GSR	2936	GAGGTGCTGAAGTTCTCCCAGGTCA	CCGGGAACTGCAGTAACCATGCTG
GSTA4	2941	AGCTCCACTATCCCAACGGA	TTCATCAAACTCGACTCCGGC
GSTZ1	2954	CCTGATTCGTCGAGTCTCACT	ATAGAGGATGGGCTTCCCCG
IGFBP3	3486	CGCGCCAGGAAATGCTAG	AATGGAGGGGGTGGAACTT

		TG	G
KEAP1	9817	CGACAACCAAGACCCCGCA	GATAAGCAACACCACCACCTCT
MAP1LC3B	81631	CCGCCTTTTTGGGTAGAAGT	AACTGTGATGGCAAATGCGT
NFE2L2	4780	CCCAACACACGGTCCACAGCTC	AATCCATGTCCTGCTGGGACGGG
NFKBIA	4792	CTTCGAGTGACTGACCCCAG	TCACCCCACATCACTGAACG
NQO1	1728	GAAAGGCTGGTTTGAGCGAG	CCTTCTTACTCCGGAAGGGT
PPAT	5471	GCTTACGCAGGAAAGTGTGG	TGGCTGAATGAAGGTTCTCCC
RGN	9104	GCCCTGTACTCCCTCTTTCC	GTGGTCTAGCGACCAATCCA
SIRT1	23411	TGCAACAGCATCTTGCCTG	AGGACATCGAGGAACTACCTGATT

Table S5. Primer sequences used for quantitative real-time PCR.